https://doi.org/10.5194/egusphere-2025-5026
Preprint. Discussion started: 5 March 2026

Suspended sediment dynamics in an urban, mountain catchment in Nepal

Rajaram Prajapati[1,6], Saroj Karki[2], Saraswati Thapa[3], Hanik Lakhe[4], Daniel J. Bain[1], John Gardner[5]

[1]Department of Geology and Environmental Science, University of Pittsburgh, Pittsburgh, USA
[2]Ministry of Water Supply, Irrigation and Energy, Biratnagar, Nepal
[3]School of Geosciences, University of Edinburgh, Edinburgh, UK
[4]Department of Water Resources and Environmental Engineering, Asian Institute of Technology, Pathum Thani, Thailand
[5]Department of Earth, Marine and Environmental Sciences, University of North Carolina at Chapel Hill, Chapel Hill, USA
[6]SmartPhones4Water, Chico, USA

Correspondence to: Rajaram Prajapati (livaraja08@gmail.com)

Abstract. Urban mountain catchments are highly vulnerable to erosion and sedimentation due to steep terrain, intense rainfall, and rapid land-use change at the urban fringe. However, event-scale sediment transport remains poorly understood in these regions, particularly in data-scarce areas such as the Himalayas. This study presents the first high-frequency, event-based analysis of suspended sediment transport in the Nakkhu River, a rapidly urbanizing catchment in Kathmandu Valley, Nepal. Using optical backscatter sensors and targeted field sampling during the 2023 monsoon, we analysed how rainfall, antecedent moisture, and human disturbance shaped sediment responses. Sediment transport was highly episodic, with two extreme storms accounting for nearly half of the seasonal suspended sediment load. Analysis of SSC–discharge hysteresis patterns revealed event-specific variability shaped by rainfall intensity, antecedent conditions, and hydrologic connectivity. Peak SSC often lagged peak discharge during low-flow events, suggesting upstream sediment sources. In contrast, high-intensity storms produced rapid sediment delivery, likely from hillslopes, mining zones, and in-channel deposits. Low-frequency (daily) monitoring underestimated sediment loads by approximately 30% compared to 30-minutes interval data. This study provides the first 30-minute interval event-scale analysis of suspended sediment transport in Kathmandu Valley, revealing how sediment responses vary across the monsoon season in relation to rainfall intensity, discharge dynamics, and antecedent conditions. These insights, including lagged sediment peaks during low-flow events and rapid sediment flushing during intense storms, highlight the value of sub-hourly monitoring for capturing within-event variability and identifying short-lived sediment sources in urban mountain watersheds.

https://doi.org/10.5194/egusphere-2025-5026
Preprint. Discussion started: 5 March 2026

1 Introduction

Sediment production rates in mountainous areas are accelerated by intense orographic precipitation, strong topographic gradients (i.e., steep terrain), and rapid/recent pressure release in the bed rock (Houvis et al., 2000; Millman and Syvitski, 1992; Slaymaker, 2018). Mobilized sediment subsequently affects downstream river morphology, reservoir capacity, aquatic ecosystems, and coastal sediment supply (Montgomery, 2001; Syvitski et al., 2005). In parallel, urban areas characterized by impervious surfaces, altered drainage networks, and rapid land-use transitions, that together tend to increase runoff and upstream erosion, often leading to elevated and erratic sediment fluxes downstream (Booth, 1991; McVey et al., 2023; Safdar et al., 2024; Walsh et al., 2005; Zarnaghsh and Husic, 2021). When mountainous terrain is urbanized, the combined effect of relief-driven erosion and anthropogenic disturbance can result in severe erosion and sedimentation. These interacting processes can overwhelm drainage infrastructure, degrade water quality, accelerate riverbed incision or aggradation, leading to altered channel capacity, and increase the risk of flash floods and sediment-related hazards, thereby posing serious challenges for watershed management, flood mitigation, and the long-term resilience of urban infrastructure.

Capturing relevant sediment transport dynamics in urban mountain catchments requires high-resolution monitoring, as runoff and sediment fluxes can shift dramatically within hours. Runoff-sediment interactions are more complex due to urban infrastructure and landscape disturbance, which alter flow paths and activate sediment from diverse sources in rapid succession. These challenges result in poorly quantified, event-scale sediment transport dynamics in urbanizing mountain catchments, particularly in resource-constrained regions. Most event-scale sediment studies in urban environments have focused on "developed" regions such as the USA, Europe, and New Zealand (Haddadchi and Hicks, 2020; Oeurng et al., 2010; Pillo et al., 2023; Safdar et al., 2024), while comparable research in rapidly urbanizing mountain catchments, such as Kathmandu Valley, largely do not exist. In Nepal, previous sediment studies have primarily relied on daily observations or modeled estimates (Pokhrel, 2018; Thapa et al., 2024a; Thapa et al., 2024b), limiting the ability to capture short-term sediment dynamics during flood events.

Kathmandu Valley, the political and economic centre of Nepal, is the country's most densely populated and rapidly urbanizing region (Ishtiaque et al., 2017; Prajapati et al., 2018). Drained by the Bagmati River, its once naturally dynamic river systems have been heavily altered by rapid urbanization and infrastructure expansion (Danegulu et al., 2024; Thapa et al., 2024b). Unregulated floodplain encroachment, hillslope road construction, and extensive sand mining have disrupted sediment pathways, constrained river flow, and intensified erosion, leading to rising sediment loads in rivers (Lamichhane et al., 2025). These anthropogenic changes, coupled with climate change-induced extreme rainfall events, have exacerbated urban flooding, which has become more frequent and severe, accelerating sediment mobilization and deposition, and posing risks to infrastructure and downstream communities (Prajapati et al., 2018; Thapa et al., 2024a). This growing vulnerability was further

https://doi.org/10.5194/egusphere-2025-5026
Preprint. Discussion started: 5 March 2026

demonstrated during the September 2024 flood-triggered by record-breaking rainfall-which led to landslides, inundated settlements, damaged infrastructure, and further caused widespread channel alteration and sediment deposition along river corridors and floodplains (Lamichhane et al., 2025).

While bedload transport is important in steep mountain rivers, we focus here on suspended sediment due to its measurability using high-frequency optical sensors (Langhorst et al., 2023) and its abundance in monsoon-fed systems (Henck et al., 2010; Qazi et al., 2018). Suspended sediment is of particular concern in urban catchments due to its dual role in transporting contaminants that impair water quality and contributing to sediment deposition that exacerbates flood risk and threatens infrastructure resilience. This study presents the first 30-min interval event-based analysis of suspended sediment transport in Kathmandu Valley, Nepal, addressing this gap and providing critical insights into how suspended sediment transport varies across the monsoon season in response to shifting event-scale drivers, including rainfall intensity, discharge, and antecedent conditions, in a rapidly changing urban watershed. Using a combination of low-cost in-situ sensors, field measurements, and citizen science, we focused on three main questions: 1) How does suspended sediment transport evolve over the course of the monsoon season in response to changing hydrological conditions in a steep, urbanizing mountainous catchment? 2) To what extent do hydrologic extremes control sediment export, and 3) How critical is high-frequency monitoring in capturing these episodic fluxes? We also examine the spatial variability of sediment sources to contextualize observed suspended sediment concentration (SSC) patterns under different hydrological conditions.

2 Methods

2.1 Study Area

The Nakkhu River sediment transport is changing due to rapid urbanization of the mountain watersheds it drains (Fig. 1). Its steep terrain, highly dynamic channel, and exposure to both natural and anthropogenic disturbances make it particularly susceptible to upstream erosion, downstream sedimentation, and variations in sediment flux (Maharjan and Tamrakar, 2010). The Nakkhu River catchment, located in the southern part of the Kathmandu Valley in central Nepal, drains approximately 52.3 km^2. The river originates in the southern hills at an elevation of around 2540 m above sea level and flows northward for 26 km before joining the Bagmati River. The catchment has an elongated shape, characterized by steep upper reaches and a relatively narrow downstream section (Fig. 1(e)), and an average channel gradient of 5.2%, and consequently has a dynamic flow regime (Maharjan and Tamrakar, 2010). The upper catchment experiences frequent landslides and extensive sand mining, while the lower reaches are increasingly affected by floodplain encroachment and urban expansion (Thapa et al., 2024a). The region experiences a subtropical monsoon climate, with four distinct seasons: pre-monsoon (March–May), monsoon (June–September), post-monsoon (October–November), and winter (December–February) (Talchabhadel et al., 2020). The Kathmandu Valley receives an average annual precipitation of approximately 1610 mm (1880 mm in mountain areas and 1410 mm on the valley floor), with over 80% occurring during the monsoon season (Prajapati et al., 2021b). Summer temperatures

https://doi.org/10.5194/egusphere-2025-5026
Preprint. Discussion started: 5 March 2026

range between 28–30°C, while winter temperatures can drop to around 0°C (Ishtiaque et al., 2017; Prajapati et al., 2021a). The lithology of the Nakkhu River catchment comprises limestone, meta-sandstone, meta-siltstone, quartzite, slate, and phyllite, with alluvial deposits found downstream near Tika Bhairab and Champi (Maharjan and Tamrakar, 2011). Gravel and sandy terraces dominate the upper catchment, reflecting active sediment mobility, while the midstream section exhibits significant sediment transport driven by uplift, erosion, and changes in slope and river energy. The low-gradient downstream experiences higher sediment deposition than the upstream region (Bhatta and Adhikari, 2024).

https://doi.org/10.5194/egusphere-2025-5026
Preprint. Discussion started: 5 March 2026

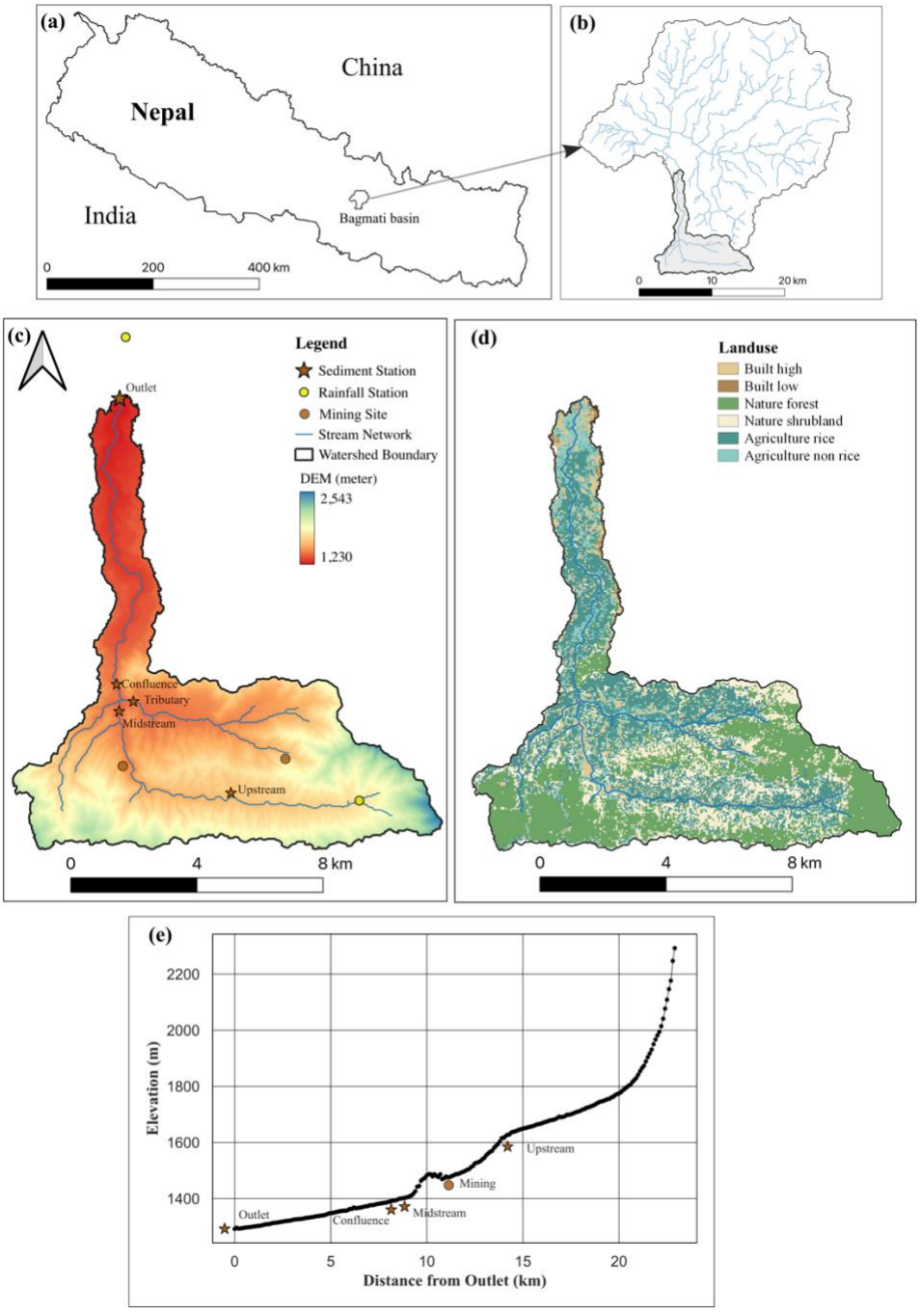

Figure 1: Overview of the study area: (a) Geographic location of the study area. (b) Bagmati River Basin within the Kathmandu Valley, highlighting the Nakkhu catchment in the south-eastern region (shaded grey). The river network is shown in blue. (c) Nakkhu catchment with a Digital Elevation Model (DEM) as the background. Rainfall and sediment monitoring stations are marked with yellow circles and brown stars, respectively. (d) Land use classification map (Davids et al., 2018). (e) Longitudinal profile of the Nakkhu River mainstem, from the upstream reach to the catchment outlet.

https://doi.org/10.5194/egusphere-2025-5026
Preprint. Discussion started: 5 March 2026

2.2 Hydro-climatological and sediment data

We collected high-resolution rainfall, discharge, and SSC data. Rainfall was monitored at 30-minute intervals using two tipping bucket rain gauges (0.2-mm resolution; Fig 1(c)). Stream stage was recorded every 30 minutes at the catchment outlet using a differential pressure transducer attached to an optical backscatter (OBS) sensor (Langhorst et al., 2023). Discharge measurements were taken twice a month using an acoustic Doppler velocimeter, and a stage-discharge rating curve was developed to estimate continuous discharge from stage data. The relationship is expressed as Eq. (1):

$$Q = 8.63 * h\text{^}1.56 \quad (1)$$

where Q is discharge (m^3/s) and h is water stage (m).

SSC was monitored using both conventional manual sampling and in situ OBS sensors. Field samples were collected three times a week and more frequently during flood events. SSC was determined gravimetrically by filtering water samples through a 0.45-micron filter, drying at 105°C, and weighing the retained sediment (Eaton and Clesceri, 1995). An OBS sensor was mounted on a bridge pier near the streambank at a depth of approximately 0.2 m from the bed to ensure submersion across varying flow conditions. The OBS sensor emits infrared light and detects the intensity of backscattered light from suspended particles in the water. Thus, measured backscatter is then calibrated to estimate continuous SSC using a regression model.

The deployment of the OBS sensor at the monitoring site posed several challenges that affected the accuracy and continuity of SSC measurements. During low-flow conditions, the sensor was exposed to ambient light, leading to anomalously high and erratic backscatter readings. To address this issue, SSC data from low-flow periods were excluded from the analysis, and only flood event data were considered. Additionally, biofouling and debris accumulation on the sensor screen periodically interfered with backscatter measurements. As a result, data from a few events were discarded due to suspected measurement errors and potentially unreliable backscatter readings.

2.3 SSC-backscatter relationship

We developed an empirical model to estimate SSC from sensor backscatter by fitting regression functions to paired measurements of backscatter and SSC. Rather than adopting a single functional form over the full dynamic range, we used a piecewise regression approach to account for the distinct behaviours observed at low and high backscatter values (Fig. 2(a)); Bunt et al., 1999; Downing, 2006; Kineke and Sternberg, 1992). While power law relationships are frequently employed in sediment monitoring studies (Oeurng et al., 2010), we found them prone to overprediction at high backscatter levels and unstable near the origin. The breakpoint for the piecewise model was determined empirically by examining the inflection zone where the log-linear trend at low SSC transitions to a near-linear relationship at higher values. A threshold of backscatter =

https://doi.org/10.5194/egusphere-2025-5026
Preprint. Discussion started: 5 March 2026

7050 provided the most consistent split, capturing the underlying change in SSC dynamics while minimizing residuals and discontinuity between the two segments. To quantify the uncertainty associated with model predictions, we applied a Monte Carlo simulation using the parameter covariance matrices from each fitted segment. For values ≤7050, SSC was modelled as an exponential function of backscatter, expressed in semi-logarithmic form (R^2 = 0.736; RMSE = 280.7 mg/l) and the 95% confidence interval was derived using 10,000 simulations. For values >7050, a linear model provided an adequate fit to the data (R^2 = 0.821; RMSE = 1584.2 mg/l), and confidence bounds were similarly estimated (Fig. 2(a)).

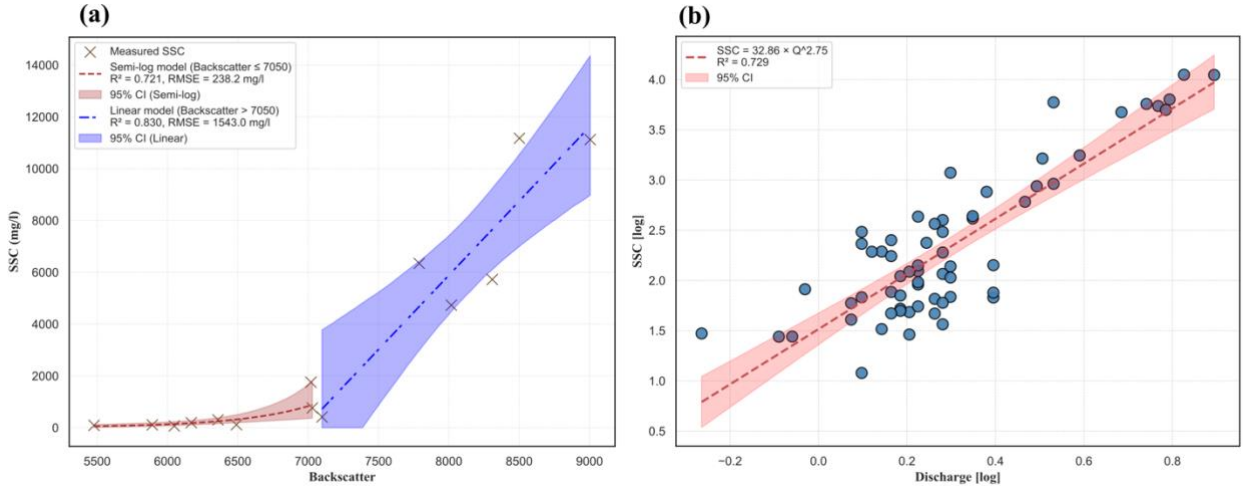

Figure 2: (a) Piecewise regression model for estimating suspended sediment concentration (SSC) from backscatter measurements. A semi-log model is used for lower values (red dashed line), while a linear model is applied for higher values (blue dashed line). Measured SSC values are shown as brown "×" markers. (b) Relationship between suspended sediment concentration (SSC) and discharge. Log–log scatterplot of SSC versus discharge, with each point representing an individual observation (blue dots). The red dashed line denotes the best-fit power-law regression line, highlighting the underlying relationship between SSC and discharge. Shaded regions represent the 95% confidence intervals derived from Monte Carlo simulations for each segment.

2.4 Event Analysis

Flood events were identified using the objective time-series analysis method developed by Giani et al. (2022), which simultaneously considers rainfall and streamflow data without requiring baseflow separation or extensive parameter adjustments. During the whole study period, between May 2023 and October 2023, there were 16 flood events, out of which we observed 9 flood events with reliable continuous measurements of backscatter.

To assess the relationship between rainfall, discharge, antecedent conditions and sediment transport, an event scale database was generated for each flood event which contained four groups of variables: antecedent conditions, rainfall, discharge and suspended sediment during the flood. Antecedent conditions included initial discharge ($Q_{initial}$) and accumulated rainfall 12 hours before flood (P0.5), 1 day before (P1), and 3 days before (P3), to capture pre-event hydrological conditions. Rainfall characteristics comprised total event rainfall, maximum rainfall intensity, and the time lag between peak discharge and peak

https://doi.org/10.5194/egusphere-2025-5026
Preprint. Discussion started: 5 March 2026

rainfall. Discharge metrics included mean and peak discharge, flood volume, flood duration, and the time to rise and fall. Suspended sediment parameters were represented by peak and mean SSC, total sediment load, and the lag time between peak SSC and peak discharge. This structured dataset allowed for detailed event-scale evaluation of sediment transport dynamics across varying hydrological conditions.

2.5 Impact of extreme events on sediment transport

The contribution of extreme flood events to total sediment transport was assessed using cumulative water volume and sediment load frequency curves. The cumulative water volume curve was constructed from half-hourly discharge data for the entire study period. The sediment load frequency curve was developed using half-hourly SSC data for the nine selected flood events. For all other periods, including non-event periods and seven flood events where reliable SSC estimates from the OBS sensor were unavailable, SSC was estimated using an SSC-discharge rating curve (Fig. 2(b)). This rating curve was derived from manual water sample SSC measurements and corresponding discharge data (Walling, 1977) and was applied to half-hourly discharge records to generate continuous SSC estimates, ensuring comprehensive sediment load calculations across both event and non-event periods.

To evaluate how sediment load estimates vary with temporal resolution, we computed sediment loads across multiple timescales, including half-hourly, hourly, 2-hourly, 4-hourly, 6-hourly, 12-hourly, daily, weekly, and monthly intervals. SSC values at daily, weekly, and monthly resolutions were generated by applying the commonly used SSC–discharge rating curve approach (Walling, 1977), developed from manual water sample data, to discharge records aggregated at corresponding timescales (Fig. 2(b)). In contrast, SSC estimates at sub-daily resolutions (half-hourly to 12-hourly) were from optical backscatter (OBS) sensor data during flood events and supplemented with sediment rating curve estimates for non-event periods. To account for model uncertainty, we applied Monte Carlo simulations based on the covariance of the fitted sediment rating curve ($\log_{10}$SSC vs. $\log_{10}$Q), propagating the uncertainty in discharge estimates through the regression to generate 95% confidence intervals around sediment load estimates (Tarras-Wahlberg and Lane, 2003) This multi-resolution comparison was designed to assess the sensitivity of sediment flux calculations to data frequency and to quantify the potential underestimation associated with lower-resolution monitoring.

2.6 SSC-discharge relationship analysis

The relationship between SSC and discharge during flood events was analysed using high-frequency sensor measurements. Hysteresis in SSC–discharge relationships occurs when peak SSC and peak discharge are not synchronized, forming distinct loop patterns that are interpreted to reflect sediment availability, source proximity, and transport efficiency (Williams, 1989). Based on the timing of peak SSC relative to peak discharge, four distinct hysteresis patterns were observed: (1) Linear – where SSC and discharge varied proportionally with no hysteresis; (2) Clockwise hysteresis – where SSC peaked before discharge; (3) Anticlockwise hysteresis – where SSC peaked after discharge; and (4) Complex hysteresis – characterized by multiple SSC

https://doi.org/10.5194/egusphere-2025-5026
Preprint. Discussion started: 5 March 2026

and discharge peaks (Oeurng et al., 2010). These patterns were determined for each flood event to examine variations in sediment transport dynamics across different hydrological conditions. To quantify the direction and magnitude of sediment hysteresis loops, we computed the Hysteresis Index (HI) following the method of Lawler et al. (2006), as applied by Pillo et al. (2023). HI compares suspended sediment concentrations on the rising and falling limbs of the hydrograph at a common discharge point (Q_{mid}), calculated as:

$$Q_{mid} = 0.5(Q_{max} - Q_{initial}) + Q_{initial} \quad (2)$$

where $Q_{initial}$ and Q_{max} are the initial and peak discharges of the event, respectively. The corresponding SSC values at Q_{mid} on the rising (SSC_{RL}) and falling (SSC_{FL}) limbs were then used to compute HI using one of two equations, depending on whether $SSC_{RL} > SSC_{FL}$ or vice versa:

If $SSC_{RL} > SSC_{FL}$:

$$HI = \frac{SSC_{RL}}{SSC_{FL}} - 1 \quad (3)$$

If $SSC_{RL} < SSC_{FL}$:

$$HI = \left(-\frac{1}{\frac{SSC_{RL}}{SSC_{FL}}}\right) + 1 \quad (4)$$

A positive HI indicates clockwise hysteresis (greater SSC on the rising limb), a negative HI indicates anticlockwise hysteresis, and values near zero reflect a symmetric or linear relationship between SSC and discharge. We calculated HI only for events with clear clockwise or anticlockwise hysteresis patterns and excluded complex events with multiple peaks, for which the method is not applicable.

Further, SSC was measured synoptically along the Nakkhu river network during select hydrological events in 2023 at five sites within an hour to provide snapshots of SSC during different hydrologic conditions. Suspended sediment samples were collected manually from the stream column, generally between the surface and mid-depth, depending on site accessibility and flow conditions. While exact sampling heights varied slightly across sites, care was taken to avoid surface skimming or near-bed sampling to minimize bias. Particle size distributions of suspended sediment were also determined from selected samples from these strategic sites using laser diffraction analysis (Syvitski, 1991) with a Beckman Coulter Particle Size Analyzer (model LS 13 320). Key grain size indices (D_{10}, D_{50}, and D_{90}) were derived to assess sediment sorting characteristics across

https://doi.org/10.5194/egusphere-2025-5026
Preprint. Discussion started: 5 March 2026

sites, where D_{10} is the particle diameter at which 10% of the sample's mass is finer (i.e., finer fraction), D_{50} represents the median particle size, and D_{90} indicates the coarser fraction with 90% of the sample finer.

3 Results

3.1 Flood events summary

The analysed events varied significantly in hydrological and sediment transport characteristics across the study period. During the study period, 16 flood events were recorded, of which 9 events were analysed - 1 in pre-monsoon and 8 in monsoon (Fig. 3). The remaining 7 events were excluded due to unreliable SSC measurements. Some flood events, such as Events 5 and 9, exhibited multiple discharge peaks during a single rainfall episode. Following Giani et al. (2022), we treated such multi-peak responses as single complex events, since discharge did not return to baseline levels and rainfall remained intermittent during the period. The duration of flood events ranged between 16 hours and 39 hours, with an average duration of 25 hours (Table 1). The flood event on August 9 took the shortest time (3 hours) to reach the peak, whereas the general rising time of floods varied from 3 hours to 14 hours, with an average of 7 hours. Peak discharge during flood events ranged from 4.03 m^3/s to 14.12 m^3/s, with an average of 7.87 m^3/s. The highest discharge was recorded on August 9, 2023, reaching 14.12 m^3/s, following a rainfall intensity of 42.4 mm/hr. Total rainfall per event ranged from 12.8 mm to 98.2 mm, with a mean of 45 mm (Table 1). Similarly, maximum rainfall intensity varied between 10.4 mm/hr and 42.4 mm/hr.

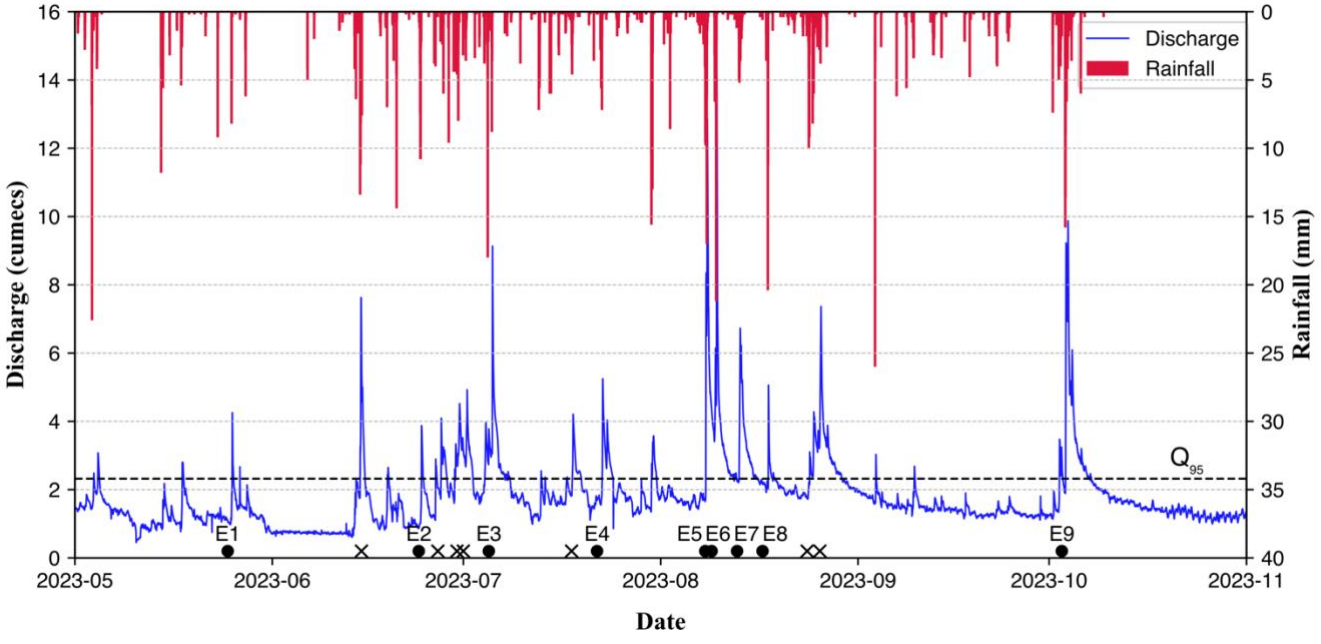

Figure 3: Time series of discharge (blue line) and rainfall (red bars) from May to October 2023, illustrating the response of discharge to rainfall events. Both rainfall and discharge are shown at half-hourly resolution. The horizontal dashed line represents the Q10 threshold. Flood events included in the analysis are labelled as E1 to E9 (black circles), while events excluded due to unreliable SSC

https://doi.org/10.5194/egusphere-2025-5026
Preprint. Discussion started: 5 March 2026

measurements are indicated by markers (x). The distribution of event labels highlights the variability in discharge responses to rainfall inputs and the selective consideration of events for sediment transport analysis.

We observed exceptionally high peak SSC during flood events that ranged from 1490 mg/l to 28200 mg/l, with a mean of 12800 mg/l. The highest peak SSC was recorded during the August 9 flood event (event 6), which also coincided with the peak rainfall intensity. Sediment load per event ranged from 100 tonnes to 6820 tonnes (mean = 1510 tonnes). While we do not have enough events with high frequency SSC and discharge for a robust statistical analysis across many events (Oeurng et al., 2010; Pillo et al., 2023; Safdar et al., 2024), detailed analysis of a limited number of well-characterized events can still reveal important patterns in suspended sediment response. Further, these data are among the first high-frequency SSC measurements in the mountain region of Nepal as well as within urbanized, mountain catchments broadly.

3.2 Event scale hysteresis and SSC dynamics

We did not find a consistent evolution of SSC-Q hysteresis from pre-monsoon to late monsoon as expected, but instead observed hysteresis patterns and event-scale SSC dynamics that related to antecedent and event hydrologic conditions. Among the nine events, four exhibited anticlockwise hysteresis (Events 1, 2, 4, and 8), one showed clockwise hysteresis (Event 7), two followed a linear pattern (Events 3 and 6), and two (Events 5 and 9) displayed complex hysteresis with multiple SSC and discharge peaks during high-intensity rainfall (Fig. 5 and Fig. A2). Peak SSC values were positively correlated with both peak discharge ($R^2 = 0.50$; Fig. 4(a)) and rainfall intensity ($R^2 = 0.80$). Further, the lag time between peak SSC and peak Q showed an inverse linear relationship with mean event discharge ($R^2 = 0.73$; Fig. 4(b)). As mean event discharge increased, peak SSC and Q grew closer in time and at the highest mean discharge SSC peaked before Q rather than after. These results suggest associations between event hydrological characteristics and sediment responses.

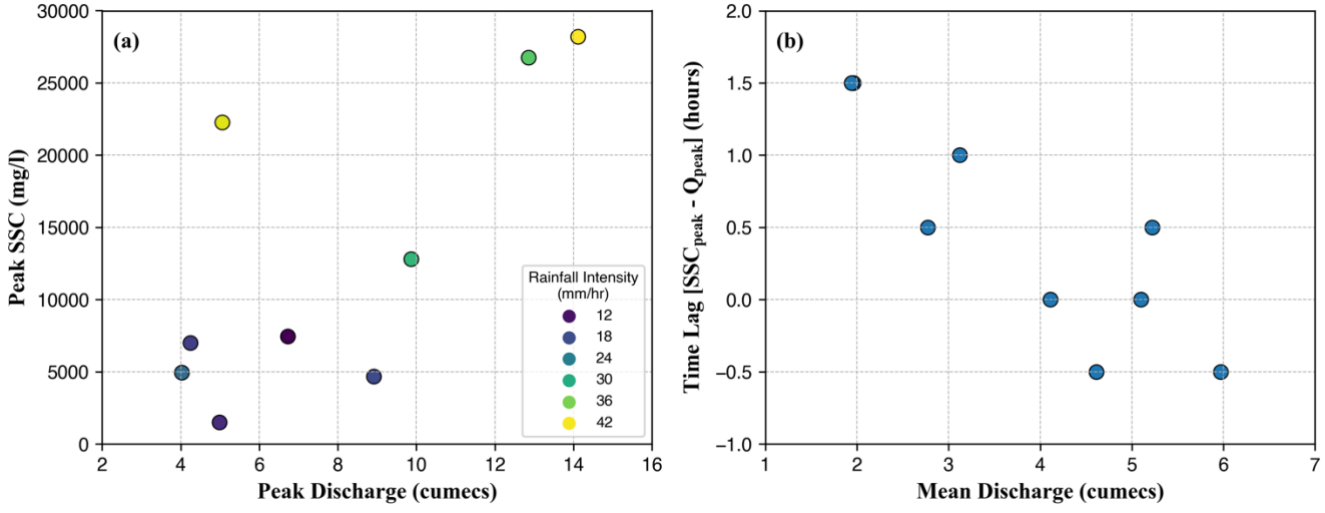

Figure 4: (a) Relationship between peak suspended sediment concentration (SSC) and peak discharge for flood events, with marker colour indicating rainfall intensity. Higher rainfall intensities tend to correspond to greater peak SSC values, suggesting a strong influence of rainfall-driven runoff on sediment transport. (b) Time lag between peak SSC and peak discharge as a function of mean

https://doi.org/10.5194/egusphere-2025-5026
Preprint. Discussion started: 5 March 2026

discharge, illustrating variability in sediment delivery timing relative to flow peaks. Positive lag times indicate that peak SSC occurs after peak discharge, highlighting the temporal complexity of sediment transport during storm events.

https://doi.org/10.5194/egusphere-2025-5026
Preprint. Discussion started: 5 March 2026

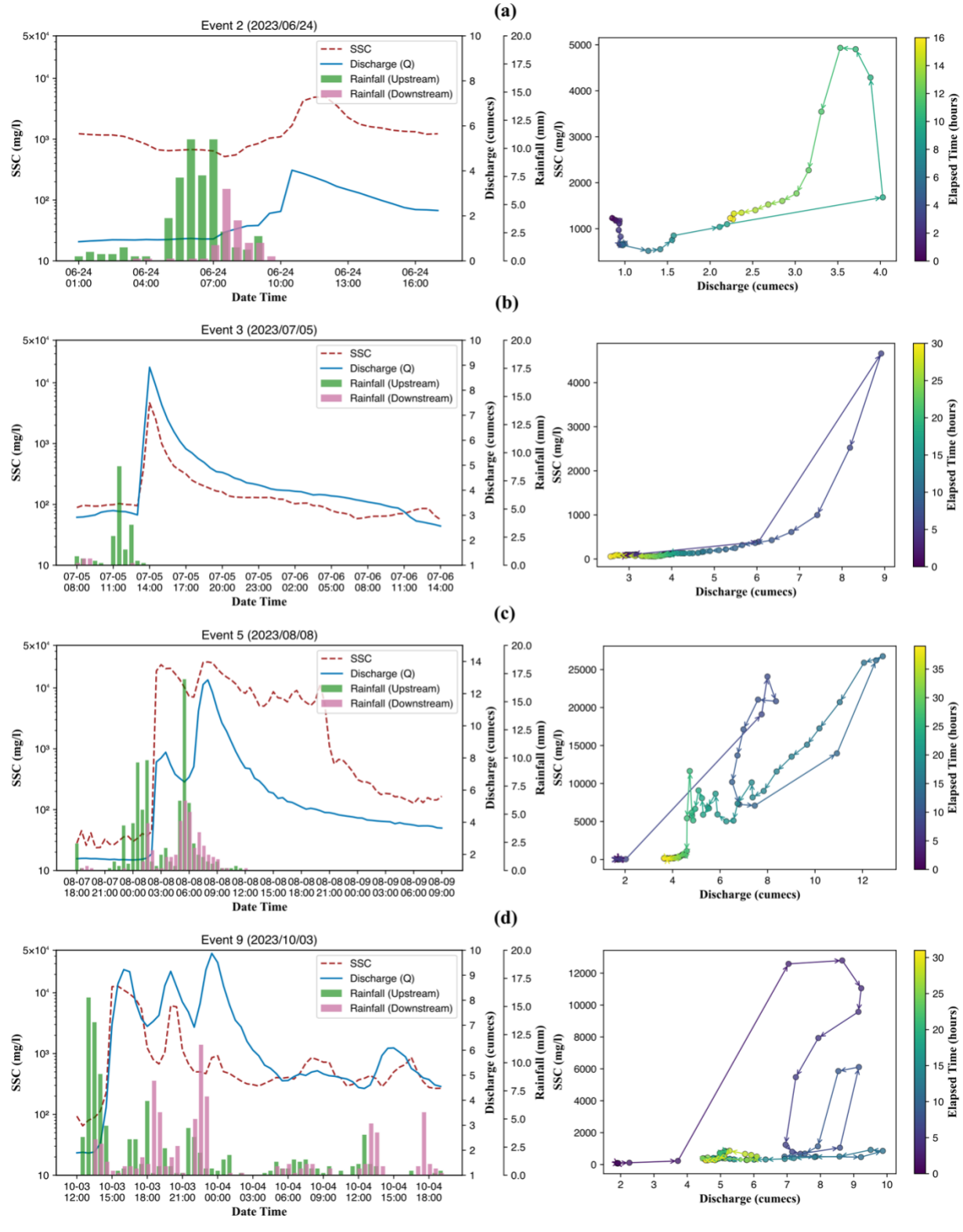

https://doi.org/10.5194/egusphere-2025-5026
Preprint. Discussion started: 5 March 2026

Figure 5: Suspended sediment dynamics and hysteresis patterns during four storm events in the Nakkhu River catchment. Left panels show event-based time series of suspended sediment concentration (SSC, dashed red line), discharge (solid blue line), and rainfall recorded at upstream (green bars) and downstream (pink bars) stations for: (a) Event 2 (2023/06/24), (b) Event 3 (2023/07/05), (c) Event 5 (2023/08/08), and (d) Event 9 (2023/10/03). The right panels display the corresponding SSC–discharge hysteresis loops coloured by elapsed time since event initiation. Marker colour represents elapsed time in hours, illustrating the evolution of sediment-discharge relationships during each storm event.

The anticlockwise hysteresis pattern observed in events 1 (pre-monsoon), 2, 4, and 8, were predominantly low-magnitude floods, occurring under dry antecedent conditions, with the lowest antecedent rainfall (P3) and initial discharge among all events. The linear SSC-discharge relationships observed in Event 3 (July 5; HI = 0.07) and Event 6 (August 9; HI = 0.1) suggest direct and proportional sediment mobilization with discharge (Table 1). Both events occurred under wet antecedent conditions, with the highest antecedent rainfall (P3) and initial discharge among all analysed flood events. In Event 3, wet antecedent conditions (P3 = 57.6 mm) and two preceding floods (June 30 and July 1) may have increased the availability of fine sediment stored in near-channel areas such as floodplain and banks, contributing to observed liner SSC-discharge relationship under moderate rainfall intensity (17.6 mm/hr) (Fig. 5(b)). In Event 6, the stream network was highly connected following the largest flood of the season (Event 5) that combined with extreme rainfall intensity (42.4 mm/hr) and led to rapid sediment mobilization. Events 5 and 9 exhibited complex hysteresis patterns, characterized by multiple peaks in both SSC and discharge that did not follow a clear clockwise or anticlockwise trajectory. Both events exhibited irregular SSC-discharge behaviour, marked by shifting sediment responses across successive discharge peaks. In Event 9, for example, the initial SSC peak preceded the discharge peak (clockwise response), followed by later phases where SSC lagged behind discharge or rose and fell in tandem with it (anticlockwise or linear segments), likely indicating shifting sediment transport mechanisms and source activation throughout the event. The gradual decline in SSC peaks despite rising discharge may be driven by downstream rainfall contributions diluting SSC rather than depletion of sediment sources (Fig. A1). The only event with a clockwise hysteresis pattern, Event 7 (August 13; HI = 0.64), had low rainfall intensity (10.4 mm/hr) coupled with high total rainfall (54.2 mm) suggesting early flushing of fine sediments stored in near-channel areas within the valley bottom, sources rather than upstream erosion.

To further illustrate within event dynamics, we highlight a few key events. Event 2 (June 24; Fig. 5(a)) was the shortest flood event (16 hours) and exhibited a delayed hydrological and sediment response despite receiving high total rainfall (51.8 mm). The event had the lowest antecedent rainfall (P3=1.4 mm) and initial discharge (0.87 m^3/s), resulting in high infiltration losses and a low runoff coefficient (0.04). Consequently, peak discharge (4.03 m^3/s) was among the lowest recorded, and the event had the lowest mean discharge (1.94 m^3/s). Notably, it was the only event where the time to rise (9.5 hours) exceeded the time to fall (6.5 hours), indicating a slow accumulation of runoff due to initial infiltration before a quicker recession phase.

The longest flood event occurred on August 8, 2023 (event 5; Fig. 5(c)), lasting 39 hours and characterized by the high total rainfall (81.0 mm) and intensity (34.0 mm/hr), resulting in peak discharge of 12.86 m^3/s and peak SSC of 26745 mg/l. The event produced the largest water yield (725,441 m^3) and transported 6824 tonnes of suspended sediment, making it the most

https://doi.org/10.5194/egusphere-2025-5026
Preprint. Discussion started: 5 March 2026

significant sediment transport event of the study period. Despite modest antecedent rainfall (P3 = 14.8 mm), elevated baseflow (1.72 m^3/s) supported efficient runoff generation. The hydrograph shows two discharge peaks from successive rainfall pulses, each closely followed by SSC peaks with minimal lag, suggesting rapid sediment mobilization.

3.3 Impact of extreme events on sediment load

A substantial proportion of the total sediment load (10,000 tons) was transported during two large flood events (Events 5 and 6), which contributed 46% of the sediment load over the study period (Fig. 6). Event 5 alone accounted for 31% (6820 tons), demonstrating the disproportionate impact of extreme events. In contrast, moderate and low-magnitude events (Events 1–4 and 7–9) each contributed less than 7%, with individual shares ranging from 0.45% (100 tons; Event 4) to 6.3% (1380 tons; Event 9). As shown in Fig. 6(a), the sediment load curve rises sharply within a short duration, indicating that a small fraction of time accounted for the majority of sediment transport. In contrast, cumulative discharge increased gradually relative to sediment load. Comparison of cumulative sediment load estimates over the six-month study period confirms that low-frequency sampling underestimates total sediment delivery. Using half-hourly SSC and discharge data, the estimated sediment load was 24,800±7860 tons over the six-month study period. In contrast, daily data yielded a substantially lower estimate of 15,700±6050 tons—an underestimate of ~37% (Fig. 7). This discrepancy becomes even more pronounced with weekly and monthly aggregations, which produced total sediment loads of 10,300±3110 and 6,400±1570 tons, respectively—nearly 58% and 74% lower than the half-hourly estimate (Fig. 7).

https://doi.org/10.5194/egusphere-2025-5026
Preprint. Discussion started: 5 March 2026

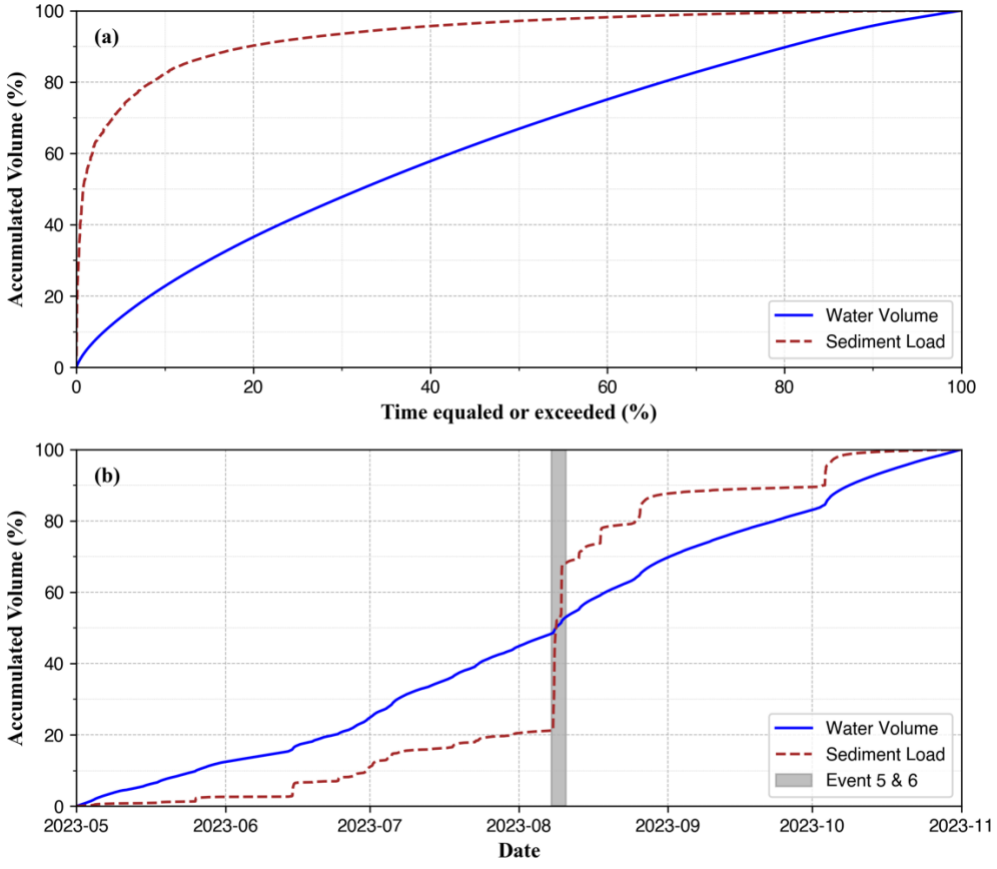

320

Figure 6: (a) Cumulative water volume and sediment load frequency curves (%) for the study period, illustrating the disproportionate contribution of high-flow events to total sediment transport. (b) Cumulative water volume and sediment load (%) over time, highlighting the episodic nature of sediment transport dominated by a few extreme flood events. The grey shaded bar indicates the combined period of Event 5 and 6, emphasizing the significant impact of these events on sediment transport.

https://doi.org/10.5194/egusphere-2025-5026
Preprint. Discussion started: 5 March 2026

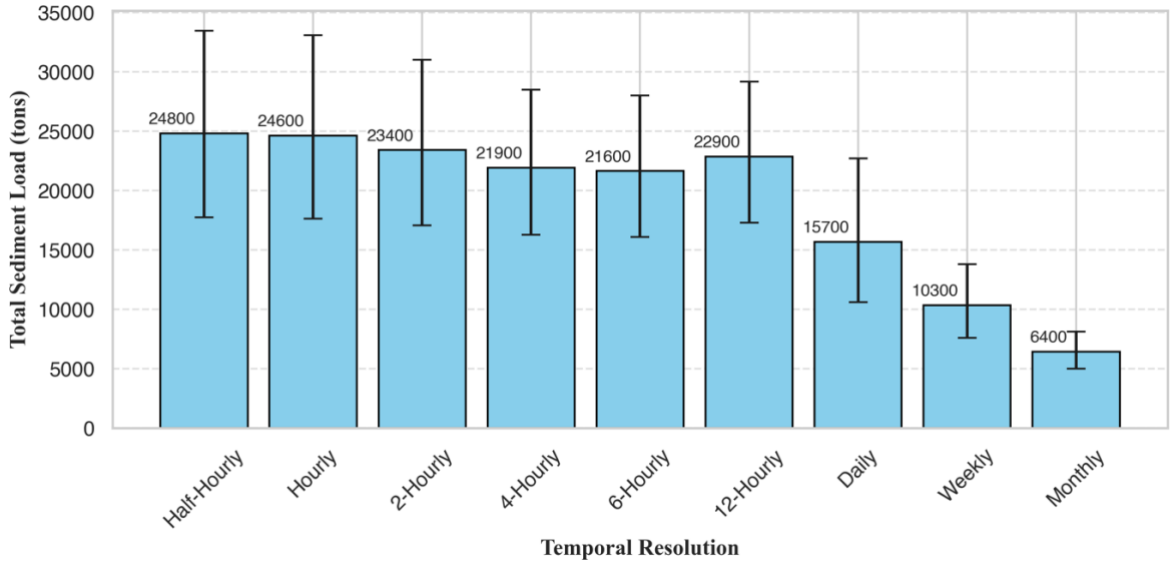

325

Figure 7: Total sediment load estimates and 95% confidence intervals across different temporal resolutions.

Table 1: Summary of key measurements from the 9 flood events.

Event	Date	Period (hours)	Rainfall (mm)	Rain Intensity (mm/hr)	Max. Q (m^3/s)	Peak SSC (mg/l)	Sediment load (tons)	Initial Q (m^3/s)	Antecedent Rainfall (P3; mm)	Hysteresis Index
1	05/25	27	14.20	16.40	4.25	6990	235	1.17	10.4	-9.38
2	06/24	16	51.80	21.60	4.03	4930	228	0.87	1.4	-0.23
3	07/05	30	19.00	17.60	8.92	4660	188	3.01	57.6	0.07
4	07/22	18	12.80	14.40	4.99	1490	100	1.68	14.4	-1.47
5	08/08	39	81.00	34.00	12.86	26750	6824	1.72	14.8	NA
6	08/09	25	37.00	42.40	14.12	28190	3206	4.82	104.6	-0.16
7	08/13	19	54.20	10.40	6.73	7440	486	2.27	7	0.64
8	08/17	17	34.80	40.80	5.06	22260	980	2.22	7	-1.92
9	10/03	31	98.20	31.60	9.87	12790	1376.7	1.96	51.8	NA

https://doi.org/10.5194/egusphere-2025-5026
Preprint. Discussion started: 5 March 2026

3.4 Sediment sources and synoptic sampling

Synoptic field measurements of SSC and grain size along the Nakkhu River network provide additional information on sediment sources. Median grain sizes (D_{50}) were finer at upstream and downstream sites (~0.018–0.020 mm) compared to midstream tributaries (~0.029–0.037 mm). Although only one particle size distribution sample was analysed per site, laser diffraction analysis has a reported precision of ±1% for D_{50} estimates, based on instrument specifications. Similarly, D_{90}–D_{10} values were smaller upstream and downstream (~0.059–0.072 mm), but midstream sites showed a broader grain size range (~0.109–0.196 mm) and poorer sorting relative to up and downstream. Synoptic SSC measurements revealed high spatial variability that changed depending on hydrological conditions (Fig. 8). During the July 23, 2023, event (Fig. 8(a)), flooding was localized in the right tributary, leading to elevated SSC at that site, while the river mainstem upstream of confluence exhibited normal flow with very low SSC. Observations indicated that the mining site located between upstream and midstream monitoring stations (Fig. 9(a)) was non-operational at this time, and water in the river mainstem upstream of the confluence appeared clear. On July 31, 2023 (Fig. 8(b)), under baseflow conditions, SSC levels were low throughout the network. However, slightly elevated SSC downstream of the mining site at midstream, compared to the upstream site, points to ongoing sediment input associated with the operational large-scale mining site (Fig. 9(a)), even in the absence of significant rainfall. The August 8, 2023, flood event (Fig. 8(c)) represented a catchment-wide response, with widespread flooding across both tributaries and the mainstem. SSC levels rose substantially at all sites, with a pronounced increase at midstream relative to upstream. Notably, in all three cases (July 23, July 31, and August 8), SSC at the catchment outlet consistently surpassed that of the confluence. Higher SSC at the outlet compared to the upstream confluence, along with longitudinal grain size patterns and field observations of in-channel sediment bars and depositional features along the main-stem (Fig. 9(d) and Table A1), suggest episodic remobilization of stored sediment from in-channel sediment sources in the urban-impacted main-stem located near the outlet.

https://doi.org/10.5194/egusphere-2025-5026
Preprint. Discussion started: 5 March 2026

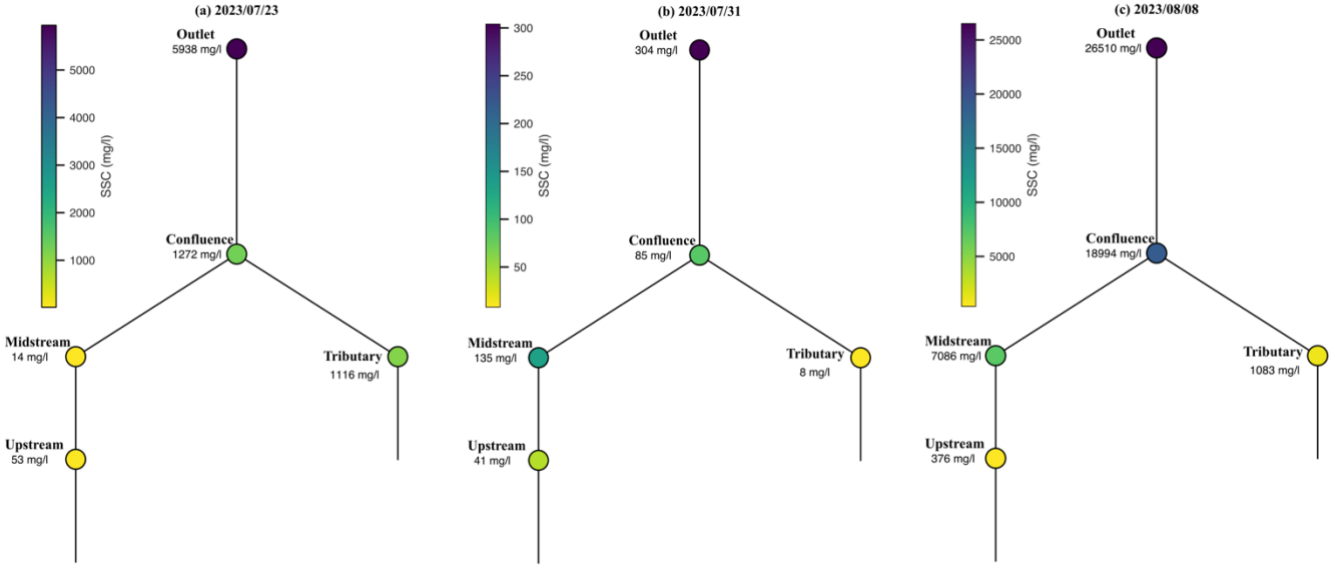

Figure 8: Longitudinal variation of suspended sediment concentration (SSC) across the Nakkhu river network under different hydrological conditions: (a) localized flooding with elevated SSC at the right tributary, (b) baseflow with slight SSC increase downstream of the mining site, and (c) catchment-wide flooding with widespread SSC increases. Each circle represents a strategic SSC monitoring site, color-coded by SSC magnitude.

https://doi.org/10.5194/egusphere-2025-5026
Preprint. Discussion started: 5 March 2026

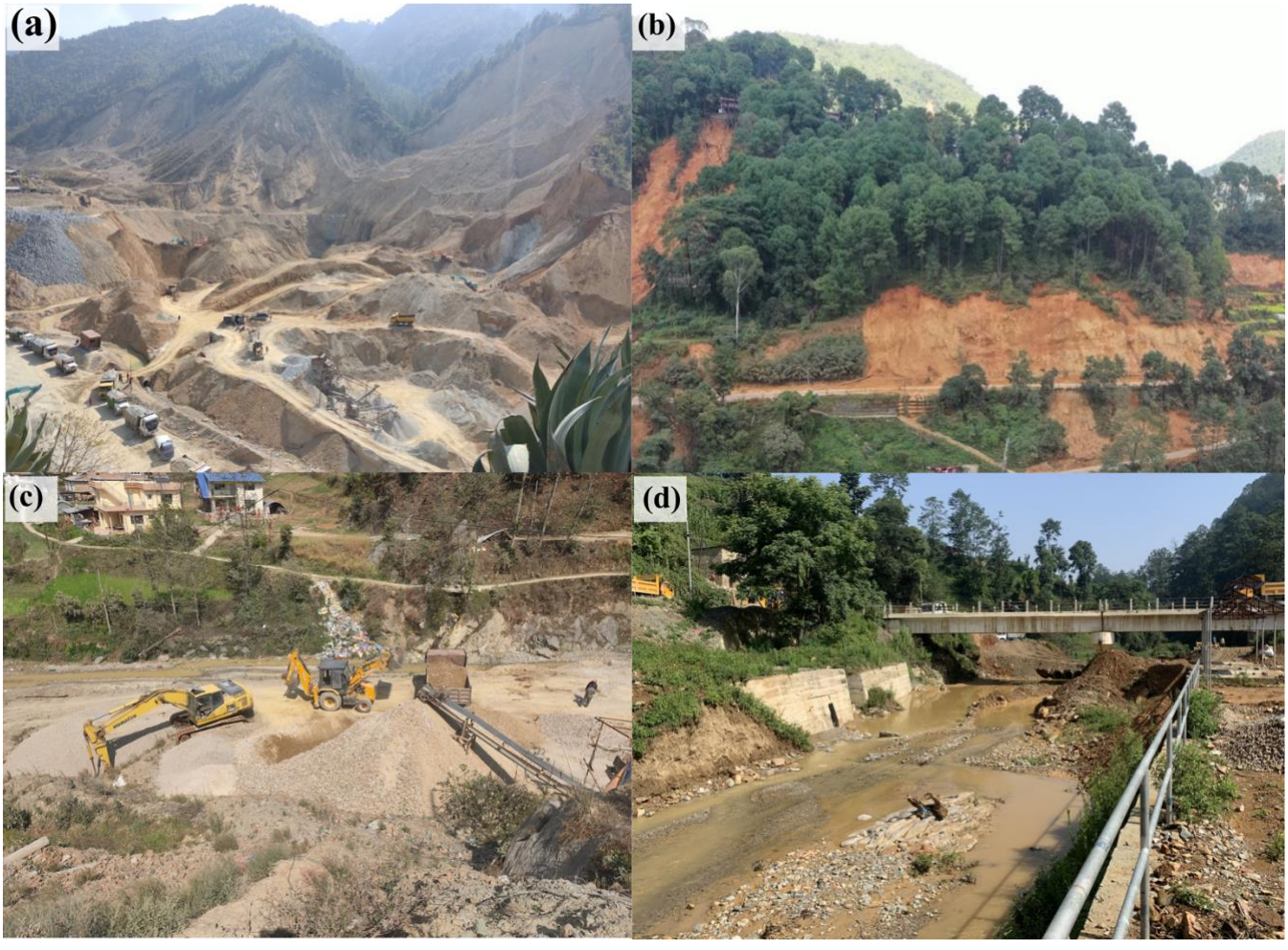

Figure 9: Field evidence of sediment sources: (a) Large-scale hillslope mining at midstream, (b) Landslide triggered by unprotected road construction, (c) In-channel riverbed sand and gravel extraction downstream of the confluence, (d) Accumulation of sediment deposits along the main river channel. Figures (b), (c), and (d) depict areas situated downstream of confluence illustrated in Figure 8.

4 Discussion

4.1 Suspended sediment transport dynamics across the monsoon season

Seasonal changes in antecedent moisture, rainfall characteristics, and hydrologic connectivity produced marked shifts in sediment transport dynamics over the monsoon period. During pre-monsoon (May) and early monsoon (June), rainfall events were often isolated and moderate in intensity, occurring during relatively dry antecedent conditions with high infiltration and low initial discharge, which reduced runoff efficiency (Merz et al., 2006b; Penna et al., 2011). Peak SSC often lagged behind peak discharge. The combination of lower discharge and counter-clockwise hysteresis suggest sediment mobilization is

https://doi.org/10.5194/egusphere-2025-5026
Preprint. Discussion started: 5 March 2026

delayed and/or derived from upstream sources (hillslopes and tributaries) or in-stream sediment deposits, but likely is not from immediate near-channel sources.

As the monsoon progressed, rainfall frequency and intensity increased and occurred during consistently wet antecedent conditions (Li et al., 2024; Merz et al., 2006a). Higher antecedent moisture conditions and higher runoff ratios could generate overland or quick flow (Vitcha et al., 2024), resulting in sharper discharge peaks and shorter response times. The observed decrease in time lag between SSC and peak discharge with increasing mean discharge (Fig. 4(b)) suggests that stronger hydrological connectivity and enhanced sediment availability reduced delays in sediment mobilization during peak monsoon floods (Masselink et al., 2017). High-intensity storms activated a broader range of sediment sources, such as landslide colluvium, unstable riverbanks, and mining sites, rapidly transporting sediment to the river channel (Ardizzone et al., 2024; Boretto et al., 2021). The highest rainfall intensities during this period triggered a series of continuous high-intensity storms, producing multiple discharge and SSC peaks within single flood events. This pattern - characterized by multiple SSC peaks closely following successive discharge peaks - suggests episodic sediment supply and efficient remobilization of available sediments. Notably, peak SSC increased with rising peak discharge, with rainfall intensity further modulating the magnitude of SSC peaks (Fig. 4(a)), indicating that both discharge capacity and storm intensity were critical factors in mobilizing sediment from diverse sources (Tuset et al., 2016). This is further exemplified by the contrast between Events 3 and 6, which had comparable cumulative water volumes (452,000 m^3 and 479,000 m^3, respectively) but vastly different sediment loads—188 tons and 3,210 tons, respectively—reflecting the amplifying effect of higher rainfall intensity and peak discharge on sediment mobilization.

Events with multiple discharge peaks, such as Event 5 and Event 9, were treated as single complex flood events following the objective event delineation method by Giani et al. (2022), which is based on combined rainfall and discharge signatures and does not require subjective baseflow separation. While this approach provides consistency and reflects the continuity of hydrometeorological forcing, we acknowledge that this choice can obscure within-event structure, particularly the timing and characteristics of individual discharge peaks that may be more influential for sediment transport in certain events. Given that our focus is on capturing the full sediment transport response associated with continuous rainfall-runoff episodes, we opted for the complex-event treatment in line with Giani et al.'s framework, which emphasizes hydrologically connected periods rather than isolated flow peaks. However, we recognize that the definition of events is not a neutral step—different approaches, such as discharge-based segmentation, may lead to different interpretations, particularly for metrics like hysteresis index. These implications should be carefully considered when comparing across studies or applying different event frameworks. Nonetheless, careful interpretation of within-event dynamics in complex flood events remains critical, as patterns of sediment transport can evolve substantially over the course of a single prolonged storm.

Complex hysteresis events such as Events 5 and 9 demonstrate the importance of within-event variability, particularly in multi-peak floods. The shifting SSC–Q relationships observed during these events—where early SSC peaks closely followed or even

https://doi.org/10.5194/egusphere-2025-5026
Preprint. Discussion started: 5 March 2026

preceded discharge peaks, and later peaks weakened or decoupled—suggest episodic sediment mobilization linked to spatially and temporally varying source activation. In Event 5, high-intensity rainfall pulses triggered successive waves of sediment input, with minimal lag, implying efficient mobilization from connected near-channel and hillslope sources throughout the event. In contrast, Event 9 illustrates how spatial rainfall heterogeneity modulates sediment availability: early upstream-driven peaks carried high sediment loads, while later downstream-driven peaks produced increased discharge but diluted SSC, likely due to limited sediment availability in downstream areas. These patterns underscore the importance of interpreting complex flood events not only as a whole but also in terms of evolving sediment source dynamics across successive rainfall-runoff phases.

The diversity of SSC–discharge hysteresis patterns observed across flood events suggests variability in sediment source proximity, sediment availability/exhaustion and transport pathways (Oeurng et al., 2010; Smith and Dragovich, 2009). Anticlockwise loops during low-magnitude floods reflect delayed sediment delivery, potentially from low antecedent moisture, limited sediment availability in downstream reaches, and weak hydrological connectivity (Baloul et al., 2024; Pillo et al., 2023). In contrast, clockwise and linear patterns were associated with wetter antecedent conditions and higher rainfall intensities, suggesting more immediate sediment mobilization from near-channel and upstream sources (Buendia et al., 2016). Complex hysteresis patterns during high-intensity storms further point to spatial variability in rainfall and sediment source activation, with multiple mobilization phases producing irregular SSC responses (Haddadchi and Hicks, 2021). Collectively, these patterns indicate that sediment transport in the study catchment was primarily transport-limited rather than supply-limited during the study period, as sediment was consistently available across events with no clear signs of exhaustion. This suggests that any future increases in rainfall intensity-whether due to climate change or a shift in monsoon dynamics-combined with human pressures such as urban expansion, riverbank modifications, land use changes, and mining activities could further amplify sediment transport, exacerbating sedimentation, flood risk and water quality degradation.

4.2 Importance of high-frequency observations

Our findings confirm that suspended sediment transport in the study catchment is highly event-driven, with extreme flood events accounting for a disproportionate share of the total sediment transport (Buendia et al., 2016; Fang et al., 2013; Ran et al., 2020a). In contrast, moderate discharge events, despite producing measurable runoff, did not mobilize large volumes of sediment, likely due to limited erosive energy and restricted sediment connectivity. This pattern is consistent with findings from other studies, which indicate that low-magnitude events primarily redistribute sediment within channels rather than export it downstream (Masselink et al., 2017; Plumb et al., 2017). The sharp rise in the sediment load curve, compared to the more gradual increase in water volume (Fig. 6), further illustrates the asynchronous and nonlinear nature of sediment delivery—highlighting that peak flows, rather than cumulative water volume, primarily govern sediment export in the study catchment. These intense storms are likely mobilizing sediment from both natural and anthropogenically disturbed hillslope sources, including shallow landslides, colluvial stores, and exposed material at active mining sites. Rainfall not only triggers hillslope

https://doi.org/10.5194/egusphere-2025-5026
Preprint. Discussion started: 5 March 2026

failures but also modulates the magnitude and timing of sediment contributions—prolonged rainfall or sequential storms can increase hillslope connectivity, expanding the extent and duration of sediment input from these sources. This concentration of sediment export within a narrow temporal window aligns with previous studies in steep, monsoon-influenced catchments, which show that 60% to 99% of annual sediment load can be transported during a few large flood events (Buendia et al., 2016; Oeurng et al., 2010; Russel et al., 2019; Leyland et al., 2017; Liu et al., 2023; Ran et al., 2020a; Ran et al., 2020b).

Based on six months of high-frequency monitoring, the study catchment's sediment yield was 420 ton/km^2, placing it on par with or exceeding annual yields reported in several high-yield Mediterranean catchments such as the Isábena (445 km^2; 530 ton/km^2; López-Tarazón et al., 2012) and the Asses (657 km^2) and Bléone (905 km^2) rivers (383 ton/km^2; Mano et al., 2009). It also surpasses long-term yields from temperate systems like the Save catchment (1,110 km^2; 70 ton/km^2; Oeurng et al., 2010) and Ribera Salada (224 km^2; 2.2 ton/km^2; Tuset et al., 2016), underscoring the high sediment delivery potential of our study catchment. While these comparisons are informative, we acknowledge that sediment transport dynamics can vary substantially across spatial scales. The Nakkhu catchment (~50 km^2) is markedly smaller than the systems cited—by a factor of 4 to 20—and this scale difference can influence both sediment supply and storage processes. Smaller catchments often exhibit more direct hillslope-channel connectivity, less in-channel sediment buffering, and faster response times to rainfall, all of which can elevate short-term sediment yield estimates. The study period occurred largely during the monsoon and likely accounts for a majority of the annual transport. The sediment yield is high, consistent with values reported for steep catchments in both wet and dry climates, reflecting a highly episodic regime driven by storm events. For much of the monitoring period, SSC remained relatively low and stable (<50 mg/l), yet during a single event (Event 5), SSC surged from 26 mg/l to 26,745 mg/l within just 14 hours. This represents more than three orders of magnitude increase over sub-daily timescales, underscoring the non-linear and episodic nature of sediment transport. Such pronounced fluctuations highlight the catchment's capacity for rapid and substantial sediment mobilization during short, high-intensity events, emphasizing the inadequacy of low-frequency sampling to capture accurate sediment loads and their dynamics.

Accurately capturing these episodic dynamics requires high-frequency monitoring (Oeurng et al., 2010, Pillo et al., 2023). In our study, sediment load estimates based on daily SSC and discharge data underestimated total sediment transport by ~37% compared to those derived from half-hourly observations. While hourly estimates aligned more closely with half-hourly values in terms of cumulative load, this apparent similarity in means and uncertainty ranges masks important differences in event-scale dynamics. Half-hourly data better resolve sharp sediment peaks and within-event variability, especially during short, high-intensity storm bursts where SSC can surge and fall rapidly. In flashy catchments like ours, even modest averaging over an hour can obscure peak sediment fluxes that contribute disproportionately to total load. For example, during Event 3 (July 5), hourly data underestimated the peak SSC by 29% and total event load by 5.9%, significantly distorting the sediment response. Similarly, in Event 1 (May 25), hourly aggregation smoothed over a sharp peak, resulting in a 15.7% drop in peak SSC and 7.1% underestimation in sediment load. Moreover, our analysis revealed that the time lag between peak SSC and

https://doi.org/10.5194/egusphere-2025-5026
Preprint. Discussion started: 5 March 2026

peak discharge was only 30 minutes for Events 6, 7, 8 and 9—lags that are entirely missed with hourly resolution. This has direct implications for interpreting hysteresis behaviour and sediment source activation, which are highly sensitive to short-lived pulses. A gradual decrease in estimated sediment load with coarser temporal resolution (Fig. 7) highlights the limitations of low-frequency monitoring, which tends to miss short-lived but sediment-rich events particularly during flashy flood events common in steep, urbanizing catchments (Francalanci et al., 2013; Safdar et al., 2024). Similar patterns have been reported in other mountainous catchments with intense seasonal rainfall. Duvert et al. (2011) showed that in small mountainous catchments (3–12 km^2), accurate yield estimates "inevitably require hourly monitoring," while daily or bi-daily schemes could lead to errors exceeding 1000%. In contrast, larger catchments (>600 km^2) allowed for less frequent sampling if timed consistently. In systems where sediment surges are tightly coupled with storm-driven runoff and anthropogenic disturbances like sand mining, missing these pulses can lead to substantial errors in sediment budgeting.

4.3 Diversity of sediment sources in urban, mountainous catchment

Synoptic sampling revealed clear spatial differences in grain size and SSC patterns along the river network, shaped by both geomorphic setting and human activities. Steep hillslopes with unprotected earthen roads (Fig. 9(b)), mining activities (Fig. 9(a) and Fig. 9(c)), widespread landslides (Fig. 9(b); Khatakho et al., 2021), and unregulated foothill excavation for housing developments without slope stabilization in the upper catchment contribute to sediment generation, particularly during high-intensity storms. Additionally, the tributaries, characterized by steep gradients, carry substantial sediment loads that are deposited at their confluence with the main river, forming debris fans, which were observed during the September 2024 flood in the study catchment (Lamichhane et al., 2025). Although 47% of the catchment is forested (Zanaga et al., 2022), with most of this cover concentrated in the upstream region (Fig. 1(d)), these areas remain highly vulnerable to erosion due to steep slopes, poor slope stability and localized human disturbances.

Synoptic sampling during different hydrological conditions further clarified the spatial dynamics of sediment delivery. During localized flooding on July 23, elevated SSC in the right tributary pointed to concentrated sediment delivery from mining deposits, disturbed hillslopes and landslides (Fig. 9(b)), as well as haphazard landad development at the hillslope–foothill interface. In contrast, during the catchment-wide August 8 flood, SSC increased substantially across all sites due to widespread sediment mobilization. Notably, the sharp increase in SSC from the upstream to the midstream site-located just downstream of an active large-scale mining site-suggests that storm-driven runoff mobilized additional sediment from the mining zone. Large-scale mining zones in the mid catchment region emerged as persistent sediment hotspots. Elevated SSC levels at this location, even in the absence of rainfall (July 31), indicate that operational mining contributes sediment independently of storm-driven runoff. Grain size patterns further support this interpretation: midstream sites consistently exhibited coarser and more poorly sorted sediments compared to the finer, more uniform particle sizes found at upstream and downstream reaches. The substantial decrease in channel slope, from 4.27% along the 5.2 km reach between the upstream monitoring site and the confluence to 1.26% along the 9 km reach between the confluence and the outlet, likely facilitates the deposition and fluvial

https://doi.org/10.5194/egusphere-2025-5026
Preprint. Discussion started: 5 March 2026

sorting of transported sediments, aligning with observed shifts in particle size distribution. The coarse and poorly sorted sediments at midstream suggest recent, localized inputs—likely from sand mining or mechanically disturbed slopes—that were deposited close to their source and have not undergone sufficient downstream transport or hydraulic sorting. In contrast, finer and more homogeneously sorted sediments suggest prolonged transport and reworking of stored bed materials or diminished transport capacity due to a reduction in slope and stream energy.

While this study provides new insight into sediment dynamics in an urbanizing mountain catchment, it is important to acknowledge certain limitations. The analysis covers a single monsoon season (May–October 2023), which may not fully capture the broader variability in sediment transport processes. Additionally, data from 7 out of 15 storm events were excluded due to unreliable SSC estimates. Still, the high-frequency observations captured key event-scale sediment dynamics, reinforcing the value of high-resolution monitoring and the need for longer-term data to support more comprehensive assessments.

5 Conclusions and Implications

This study provides the first high-frequency, event-scale assessment of suspended sediment transport in a rapidly urbanizing mountain catchment of the Kathmandu Valley. Sediment transport was highly event-driven, with two intense monsoon storms contributing nearly half of the seasonal sediment load, highlighting the dominance of extreme events in sediment transport. Sediment mobilization was shaped by a combination of rainfall intensity, antecedent moisture, and catchment disturbance, with event-scale variability reflected in diverse SSC-discharge hysteresis patterns. Several events exhibited delayed sediment peaks, indicating limited sediment availability in downstream reaches and mobilization from upstream or midstream sources. Synoptic sampling and grain size data provided further evidence that midstream mining zones and disturbed foothill areas are key sediment contributors.

These findings have important implications for urban watershed management in rapidly urbanizing and highly flood-prone mountain regions like Kathmandu Valley. The combination of natural hydrologic extremes and human-induced disturbances—such as sand mining and unregulated development—amplifies sediment-related risks to infrastructure, water quality, and ecosystem stability. Effective management will require both targeted source control (e.g., erosion mitigation and mining regulation) and improved flood discharge infrastructure. Strategies that prioritize regulating sand mining, controlling slope disturbance from road construction and haphazard land plotting at the foothills, and integrating sediment risk assessments into urban development planning are effective interventions in these cases. Such targeted interventions are vital to reducing sediment mobilization during extreme events, averting sediment hazards and consequently strengthening the flood resilience of urban mountain watersheds.

https://doi.org/10.5194/egusphere-2025-5026
Preprint. Discussion started: 5 March 2026

Appendices

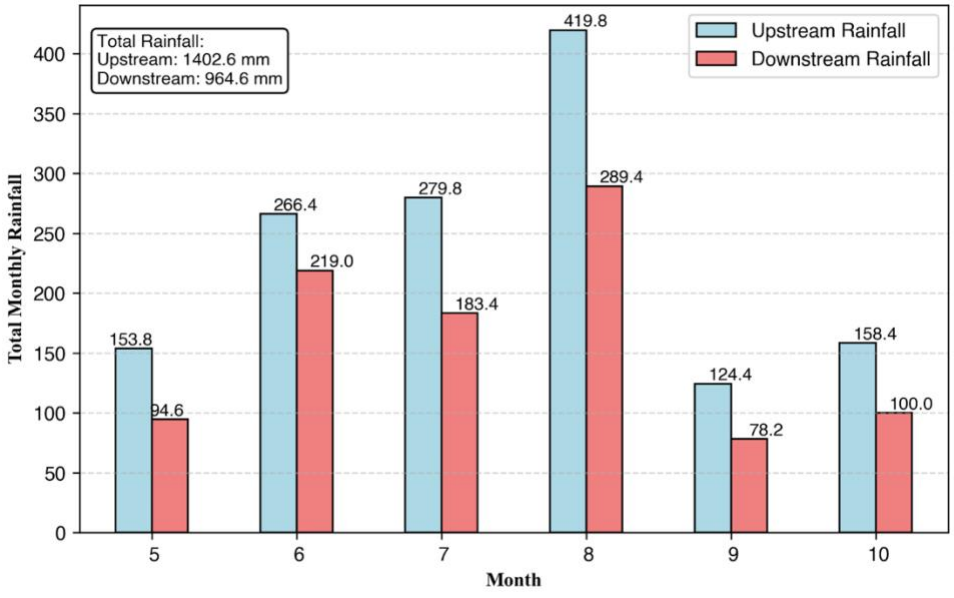

Figure A1: Monthly rainfall totals at upstream and downstream stations. Bars represent paired observations for each month, with blue and coral indicating upstream and downstream sites, respectively. Total rainfall amounts are summarized in the inset box.

https://doi.org/10.5194/egusphere-2025-5026
Preprint. Discussion started: 5 March 2026

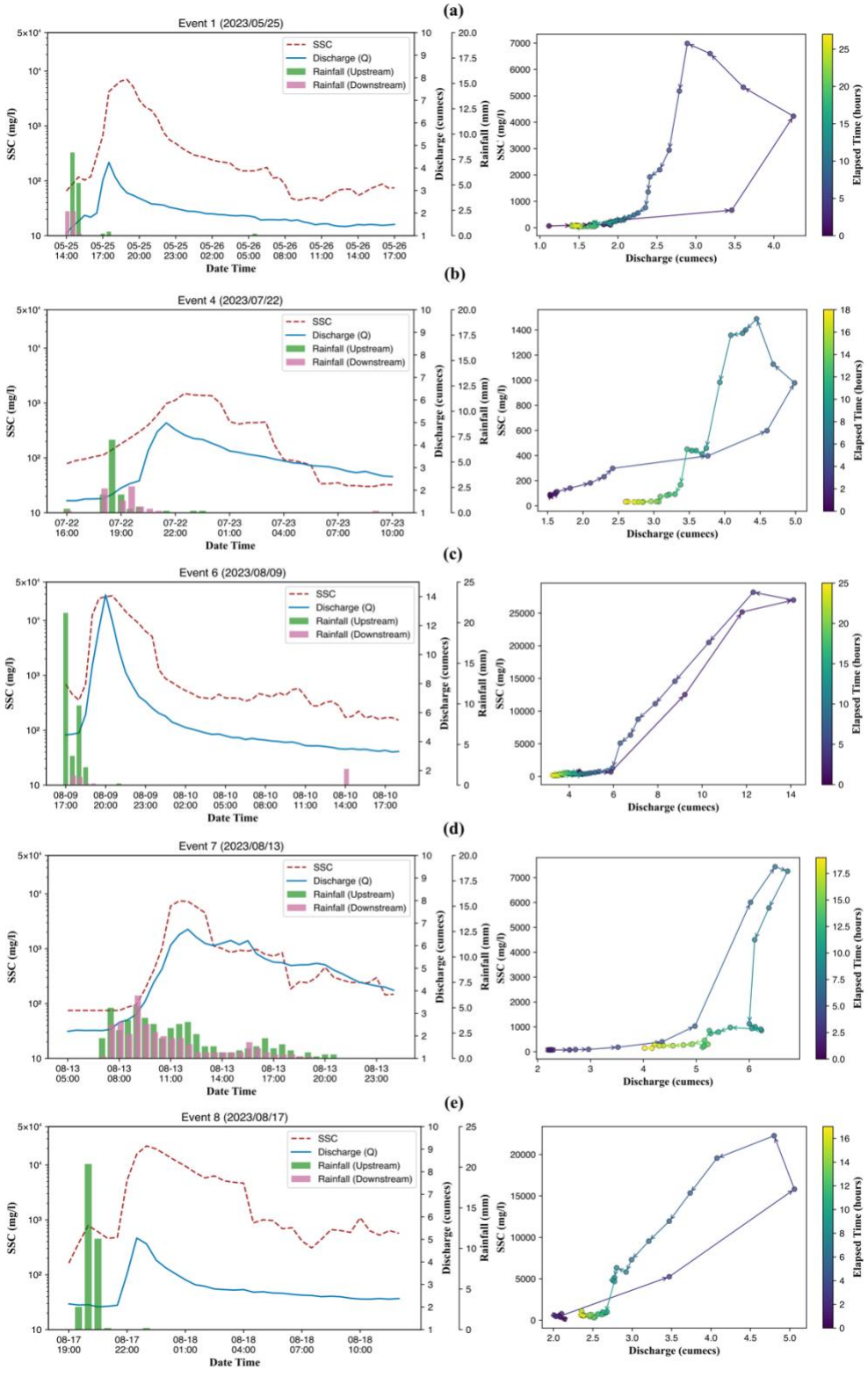

https://doi.org/10.5194/egusphere-2025-5026
Preprint. Discussion started: 5 March 2026

Figure A2: Suspended sediment dynamics and hysteresis patterns during four storm events in the Nakkhu River catchment. Left panels show event-based time series of suspended sediment concentration (SSC, dashed red line), discharge (solid blue line), and rainfall recorded at upstream (green bars) and downstream (pink bars) stations for: (a) Event 1 (2023/05/05), (b) Event 4 (2023/07/22), (c) Event 6 (2023/08/09), (d) Event 7 (2023/08/13), and (e) Event 8 (2023/08/17). Right panels display the corresponding SSC–discharge hysteresis loops colored by elapsed time since event initiation. Marker colour represents elapsed time in hours, illustrating the evolution of sediment-discharge relationships during each storm event.

Table A2: Particle size distribution for strategic monitoring sites.

Site	D_{10} (mm)	D_{50} (mm)	D_{90} (mm)	D_{90}-D_{10} (mm)
Outlet	0.00324	0.01759	0.06243	0.05919
Tributary	0.00518	0.03689	0.11413	0.10895
Midstream	0.00493	0.02939	0.20111	0.19618
Upstream	0.00349	0.02015	0.07515	0.07166

Code availability

The custom scripts used in this study are available from the corresponding author upon reasonable request.

Data availability

The data that support the findings of this study are available from the corresponding author, [author initials], upon reasonable request.

Author contribution

R.P., H.L., and J.G. conceptualized the study. R.P. designed the methodology, and R.P. and H.L. performed the data collection and analysis. R.P. wrote the original manuscript. J.G., S.K., and S.T. contributed to data interpretation and methodological refinement. J.G. supervised the project and provided critical revisions. S.K., S.T. and D.B. assisted with manuscript revisions. All authors contributed to manuscript editing and approved the final version.

Competing interests

The authors declare that they have no conflict of interest.

https://doi.org/10.5194/egusphere-2025-5026
Preprint. Discussion started: 5 March 2026

Acknowledgement

We would like to sincerely acknowledge the support provided by Smartphones For Water Nepal (S4W-Nepal). The study has been made possible by the cooperation and active involvement of S4W-Nepal citizen scientists and team members across the Kathmandu Valley. Their support in carrying out the study is gratefully acknowledged. We would also like to thank Sudeep Duwal, Rohinee Bishwas, Pratik Khanal, and Sanjiv Neupane for their assistance. This work was further supported by NASA-Earth Science New Investigator Program, NSF-EAR Postdoctoral Fellowship, the Department of Geology and Environmental Science, University of Pittsburgh and CUAHSI Pathfinder Fellowship 2023.

Financial support

Funding to Rajaram Prajapati from the NASA-Earth Science New Investigator Program Grant 80NSSC21K0921. Funding to John Gardner from NSF-EAR Postdoctoral Fellowship Grant 1806983. Fieldwork supported by the Department of Geology and Environmental Science, University of Pittsburgh and CUAHSI Pathfinder Fellowship 2023.

References

Ardizzone, F., Esposito, G., Cavalli, M., Crema, S., and Fiorucci, F.: Sediment connectivity as a key to understand geomorphic effects of the Storm Alex in two mountain catchments of the Mediterranean Alps (Italy), Geomorphology, 455, 109176, https://doi.org/10.1016/j.geomorph.2023.109176, 2024.

Baloul, D., Ghenim, A. N., and Megnounif, A.: Q–SSC behavior during floods in the Isser watershed (North-West of Algeria), Pol. J. Environ. Stud., 33, 5567–5576, https://doi.org/10.15244/pjoes/182040, 2024.

Bhatta, S. and Adhikari, B. R.: Landslide susceptibility mapping using GIS-based statistical models and remote sensing in the Kathmandu Valley, Nepal, J. Eng. Issues Solut., 3, 145–161, 2024.

Booth, D. B.: Urbanization and the natural drainage system – impacts, solutions, and prognoses, Northwest Environ. J., 7, 93–118, 1991.

Boretto, G., Crema, S., Marchi, L., Monegato, G., Arziliero, L., and Cavalli, M.: Assessing the effect of the Vaia storm on sediment source areas and connectivity in the Liera catchment (Dolomites), EGU General Assembly, EGU21-7643, 2021.

Buendia, C., Vericat, D., Batalla, R. J., and Gibbins, C. N.: Temporal dynamics of sediment transport and transient in-channel storage in a highly erodible catchment, Land Degrad. Dev., 27, 1045–1063, 2016.

https://doi.org/10.5194/egusphere-2025-5026
Preprint. Discussion started: 5 March 2026

Bunt, J. A., Larcombe, P., and Jago, C. F.: Quantifying the response of optical backscatter devices and transmissometers to variations in suspended particulate matter, Cont. Shelf Res., 19, 1199–1220, 1999.

Danegulu, A., Karki, S., Bhattarai, P. K., and Pandey, V. P.: Characterizing urban flooding in the Kathmandu Valley, Nepal: the influence of urbanization and river encroachment, Nat. Hazards, 120, 10923–10947, 2024.

Davids, J. C., Rutten, M. M., Shah, R. D. T., Shah, D. N., Devkota, N., Izeboud, P., and Van de Giesen, N.: Quantifying the connections—linkages between land-use and water in the Kathmandu Valley, Nepal, Environ. Monit. Assess., 190, 304, 2018.

Downing, J.: Twenty-five years with OBS sensors: the good, the bad, and the ugly, Cont. Shelf Res., 26, 2299–2318, 2006.

Duvert, C., Gratiot, N., Némery, J., Burgos, A., and Navratil, O.: Sub-daily variability of suspended sediment fluxes in small mountainous catchments – implications for community-based river monitoring, Hydrol. Earth Syst. Sci., 15, 703–713, https://doi.org/10.5194/hess-15-703-2011, 2011.

Eaton, C. R., and Clesceri, L. S. (Eds.): Standard methods for the examination of water and wastewater, 19th edn., American Public Health Association, Washington, D.C., Sect. 2–8, 2130 pp., 1995.

Fang, N. F., Shi, Z. H., Yue, B. J., and Wang, L.: The characteristics of extreme erosion events in a small mountainous watershed, PLoS One, 8(10), e76610, 2013.

Francalanci, S., Paris, E., and Solari, L.: A combined field sampling-modeling approach for computing sediment transport during flash floods in a gravel-bed stream, Water Resour. Res., 49(10), 6642–6655, 2013.

Giani, G., Tarasova, L., Woods, R. A., and Rico-Ramirez, M. A.: An objective time-series-analysis method for rainfall-runoff event identification, Water Resour. Res., 58, e2021WR031283, 2022.

Haddadchi, A., and Hicks, M.: Interpreting event-based suspended sediment concentration and flow hysteresis patterns, J. Soils Sediments, 21, 592–612, 2021.

Haddadchi, A., and Hicks, M.: Understanding the effect of catchment characteristics on suspended sediment dynamics during flood events, Hydrol. Process., 34, 1558–1574, 2020.

https://doi.org/10.5194/egusphere-2025-5026
Preprint. Discussion started: 5 March 2026

Henck, A. C., Montgomery, D. R., Huntington, K. W., and Liang, C.: Monsoon control of effective discharge, Yunnan and Tibet, Geology, 38, 975–978, https://doi.org/10.1130/G30886.1, 2010.

Hovius, N., Stark, C. P., Hao-Tsu, C., and Jiun-Chuan, L.: Supply and removal of sediment in a landslide-dominated mountain belt: Central Range, Taiwan, J. Geol., 108, 73–89, https://doi.org/10.1086/314387, 2000.

Ishtiaque, A., Shrestha, M., and Chhetri, N.: Rapid urban growth in the Kathmandu Valley, Nepal: monitoring land use land cover dynamics of a Himalayan city with Landsat imageries, Environ., 4, 72, 2017.

Khatakho, R., Gautam, D., Aryal, K. R., Pandey, V. P., Rupakhety, R., Lamichhane, S., and Adhikari, R.: Multi-hazard risk assessment of Kathmandu Valley, Nepal, Sustainability, 13(10), 5369, 2021.

Kineke, G. C., and Sternberg, R. W.: Measurements of high concentration suspended sediments using the optical backscatterance sensor, Mar. Geol., 108(3–4), 253–258, 1992.

Lamichhane, K., Karki, S., Sharma, K., Khadka, B., Acharya, B., Biswakarma, K., and Bhattarai, P. K.: Unraveling the causes and impacts of increasing flood disasters in the Kathmandu Valley: lessons from the unprecedented September 2024 floods, Nat. Hazards Res., 2025.

Langhorst, T., Pavelsky, T., Eidam, E., Cooper, L., Davis, J., Spellman, K., and Gleason, C.: Increased scale and accessibility of sediment transport research in rivers through practical, open-source turbidity and depth sensors, Nat. Water, 1, 760–768, 2023.

Lawler, D. M., Petts, G. E., Foster, I. D., and Harper, S.: Turbidity dynamics during spring storm events in an urban headwater river system: the Upper Tame, West Midlands, UK, Sci. Total Environ., 360, 109–126, https://doi.org/10.1016/j.scitotenv.2005.08.032, 2006.

Leyland, J., Hackney, C. R., Darby, S. E., Parsons, D. R., Best, J. L., Nicholas, A. P., Aalto, R., and Lague, D.: Extreme flood-driven fluvial bank erosion and sediment loads: direct process measurements using integrated mobile laser scanning (MLS) and hydro-acoustic techniques, Earth Surf. Process. Landf., 42, 334–346, https://doi.org/10.1002/esp.4063, 2017.

Li, J., Wu, Y., Birch, C., Schwendike, J., Graham, A., and Berry, G.: A comparison of intense rainfall characteristics and mechanisms between monsoon onset and retreat over the Yangtze River Basin, J. Water Clim. Change, 15, 3828–3849, 2024.

https://doi.org/10.5194/egusphere-2025-5026
Preprint. Discussion started: 5 March 2026

Liu, S., Wang, D., Miao, W., Wang, Z., Zhang, P., and Li, D.: Characteristics of runoff and sediment load during flood events in the Upper Yangtze River, China, J. Hydrol., 620, 129433, 2023.

López-Tarazón, J. A., Batalla, R. J., Vericat, D., and Francke, T.: The sediment budget of a highly dynamic mesoscale catchment: the River Isábena, Geomorphology, 138, 15–28, https://doi.org/10.1016/j.geomorph.2011.08.020, 2012.

Maharjan, B., and Tamrakar, N. K.: Morpho-hydraulic parameters and existing stability condition of Nakhu River, southern Kathmandu, Central Nepal, Bull. Dep. Geol., 13, 1–12, 2010.

Mano, V., Némery, J., Belleudy, P., and Poirel, A.: Assessment of suspended sediment transport in four alpine watersheds (France): influence of the climatic regime, Hydrol. Process., 23, 777–792, https://doi.org/10.1002/hyp.7178, 2009.

Masselink, R. J., Heckmann, T., Temme, A. J., Anders, N. S., Gooren, H. P., and Keesstra, S. D.: A network theory approach for a better understanding of overland flow connectivity, Hydrol. Process., 31, 207–220, 2017.

McVey, I., Michalek, A., Mahoney, T., and Husic, A.: Urbanization as a limiter and catalyst of watershed-scale sediment transport: insights from probabilistic connectivity modeling, Sci. Total Environ., 894, 165093, https://doi.org/10.1016/j.scitotenv.2023.165093, 2023.

Merz, J., Dangol, P. M., Dhakal, M. P., Dongol, B. S., and Weingartner, R.: Rainfall amount and intensity in a rural catchment of the middle mountains, Nepal, Hydrol. Sci. J., 51, 127–143, 2006a.

Merz, R., Blöschl, G., and Parajka, J.: Spatio-temporal variability of event runoff coefficients, J. Hydrol., 331, 591–604, 2006b.

Milliman, J. D., and Syvitski, J. P. M.: Geomorphic/tectonic control of sediment discharge to the ocean: the importance of small mountainous rivers, J. Geol., 100, 525–544, https://doi.org/10.1086/629606, 1992.

Montgomery, D. R.: Slope distributions, threshold hillslopes, and steady-state topography, Am. J. Sci., 301, 432–454, https://doi.org/10.2475/ajs.301.4-5.432, 2001.

Oeurng, C., Sauvage, S., and Sánchez-Pérez, J. M.: Dynamics of suspended sediment transport and yield in a large agricultural catchment, southwest France, Earth Surf. Process. Landf., 35, 1289–1301, 2010.

https://doi.org/10.5194/egusphere-2025-5026
Preprint. Discussion started: 5 March 2026

Penna, D., Tromp-van Meerveld, H. J., Gobbi, A., Borga, M., and Dalla Fontana, G.: The influence of soil moisture on threshold runoff generation processes in an alpine headwater catchment, Hydrol. Earth Syst. Sci., 15, 689–702, 2011.

Pillo, R. D., De Girolamo, A. M., Porto, A. L., and Todisco, M. T.: Detecting the drivers of suspended sediment transport in an intermittent river: an event-based analysis, Catena, 222, 106881, 2023.

Plumb, B. D., Annable, W. K., Thompson, P. J., and Hassan, M. A.: The impact of urbanization on temporal changes in sediment transport in a gravel bed channel in southern Ontario, Canada, Water Resour. Res., 53(10), 8443–8458, 2017.

Pokhrel, B. K.: Impact of land use change on flow and sediment yields in the Khokana Outlet of the Bagmati River, Kathmandu, Nepal, Hydrology, 5, 22, 2018.

Prajapati, R., Thapa, B. R., and Talchabhadel, R.: What flooded Bhaktapur, My Republica, 17, 2018.

Prajapati, R., Talchabhadel, R., Silwal, P., Upadhyay, S., Ertis, B., Thapa, B. R., and Davids, J. C.: Less rain and rainy days—lessons from 45 years of rainfall data (1971–2015) in the Kathmandu Valley, Nepal, Theor. Appl. Climatol., 145, 1369–1383, 2021a.

Prajapati, R., Upadhyay, S., Talchabhadel, R., Thapa, B. R., Ertis, B., Silwal, P., and Davids, J. C.: Investigating the nexus of groundwater levels, rainfall and land use in the Kathmandu Valley, Nepal, Groundwater Sustain. Dev., 14, 100584, 2021b.

Qazi, N. Q., and Rai, S. P.: Spatio-temporal dynamics of sediment transport in Lesser Himalayan catchments, India, Hydrol. Sci. J., 63, 50–62, https://doi.org/10.1080/02626667.2017.1409895, 2018.

Ran, L., Yang, X., Tian, M., Shi, H., Liu, S., Yu, R., and Zhou, Y.: Riverine export of water, sediment and carbon during flood events in the arid to semi-arid Wuding River on the Chinese Loess Plateau, Earth Surf. Process. Landf., 45, 1777–1788, https://doi.org/10.1002/esp.4854, 2020a.

Ran, Q., Zong, X., Ye, S., Gao, J., and Hong, Y.: Dominant mechanism for annual maximum flood and sediment events generation in the Yellow River basin, Catena, 187, 104376, https://doi.org/10.1016/j.catena.2019.104376, 2020b.

Russell, K. L., Vietz, G. J., and Fletcher, T. D.: Urban sediment supply to streams from hillslope sources, Sci. Total Environ., 653, 684–697, 2019.

https://doi.org/10.5194/egusphere-2025-5026
Preprint. Discussion started: 5 March 2026

Safdar, S., Jefferson, A. J., Costello, D. M., and Blinn, A.: Urbanization and suspended sediment transport dynamics: a comparative study of watersheds with varying degree of urbanization using concentration–discharge hysteresis, ACS EST Water, 4, 3904–3917, 2024.

Slaymaker, O.: A global perspective on denudation data, primarily specific sediment yield in mountainous regions, Landf. Anal., 36, 19–31, 2018.

Smith, H. G., and Dragovich, D.: Interpreting sediment delivery processes using suspended sediment–discharge hysteresis patterns from nested upland catchments, south-eastern Australia, Hydrol. Process., 23, 2415–2426, 2009.

Syvitski, J. P. M., Vörösmarty, C. J., Kettner, A. J., and Green, P.: Impact of humans on the flux of terrestrial sediment to the global coastal ocean, Science, 308, 376–380, https://doi.org/10.1126/science.1109454, 2005.

Syvitski, J. P. (Ed.): Principles, methods, and application of particle size analysis, Cambridge University Press, Cambridge, 1991.

Talchabhadel, R., Nakagawa, H., Kawaike, K., and Prajapati, R.: Evaluating the rainfall erosivity (R-factor) from daily rainfall data: an application for assessing climate change impact on soil loss in Westrapti River basin, Nepal, Model. Earth Syst. Environ., 6, 1741–1762, 2020.

Tarras-Wahlberg, N. H., and Lane, S. N.: Suspended sediment yield and metal contamination in a river catchment affected by El Niño events and gold mining activities: the Puyango River basin, southern Ecuador, Hydrol. Process., 17(15), 3101–3123, 2003.

Thapa, S., Sinclair, H. D., Creed, M. J., Borthwick, A. G., Watson, C. S., and Muthusamy, M.: Sediment transport and flood risk: impact of newly constructed embankments on river morphology and flood dynamics in Kathmandu, Nepal, Water Resour. Res., 60, e2024WR037742, 2024a.

Thapa, S., Sinclair, H. D., Creed, M. J., Mudd, S. M., Attal, M., Borthwick, A. G., and Watson, C. S.: The impact of sediment flux and calibre on flood risk in the Kathmandu Valley, Nepal, Earth Surf. Process. Landf., 49, 706–727, 2024b.

Tuset, J., Vericat, D., and Batalla, R. J.: Rainfall, runoff and sediment transport in a Mediterranean mountainous catchment, Sci. Total Environ., 540, 114–132, 2016.

https://doi.org/10.5194/egusphere-2025-5026
Preprint. Discussion started: 5 March 2026

Vichta, T., Deutscher, J., Hemr, O., Tomášová, G., Žižlavská, N., Brychtová, M., Bajer, A., and Shukla, M. K.: Combined effects of rainfall–runoff events and antecedent soil moisture on runoff generation processes in an upland forested headwater area, Hydrol. Process., 38, e15216, 2024.

Walling, D. E.: Assessing the accuracy of suspended sediment rating curves for a small basin, Water Resour. Res., 13(3), 531–538, 1977.

Walsh, C. J., Roy, A. H., Feminella, J. W., Cottingham, P. D., Groffman, P. M., and Morgan, R. P.: The urban stream syndrome: current knowledge and the search for a cure, J. N. Am. Benthol. Soc., 24, 706–723, https://doi.org/10.1899/04-028.1, 2005.

Williams, G. P.: Sediment concentration versus water discharge during single hydrologic events in rivers, J. Hydrol., 111, 89–106, 1989.

Zanaga, D., Van De Kerchove, R., Daems, D., De Keersmaecker, W., Brockmann, C., Kirches, G., Wevers, J., Cartus, O., Santoro, M., Fritz, S., Lesiv, M., Herold, M., Tsendbazar, N. E., Xu, P., Ramoino, F., and Arino, O.: ESA WorldCover 10 m 2021 v200, Zenodo, https://doi.org/10.5281/zenodo.7254221, 2022.

Zarnaghsh, A., and Husic, A.: Degree of anthropogenic land disturbance controls fluvial sediment hysteresis, Environ. Sci. Technol., 55, 13737–13748, https://doi.org/10.1021/acs.est.1c03186, 2021.